Raman-active phonons and mode softening in superconducting $HgBa_2CuO_{4+\delta}$

M.C. Krantz,* C. Thomsen, Hj. Mattausch, and M. Cardona
Max-Planck-Institut für Festkörperforschung, Heisenbergstrasse 1, D-70569 Stuttgart, Federal Republic of Germany
(Received 9 February 1994)

Polarized micro-Raman spectra of a single crystallite of $HgBa_2CuO_{4+\delta}$ have been measured and used to assign phonon modes of A_{1g} and E_g symmetry intrinsic to the superconducting phase. Predictions of the peak positions, linewidths, and Raman cross sections from compounds with similar bonding, i.e., HgO, Y-124, and Y-123, are closely matched and suggest assignments of the high-frequency A_{1g} modes at 592 and 568 cm^{-1} to apical oxygen stretch vibrations of the ideal structure and of a Cu or O defect (in the Hg plane). The low-frequency 168, 161, and 75 cm^{-1} modes are assigned to O and Ba vibrations of E_g, A_{1g}, and E_g, symmetry, respectively. An anomaly in the phonon frequency and linewidth of the 568-cm^{-1} A_{1g} mode is observed below T_c. If interpreted as a change in the phonon self-energy due to the onset of superconductivity, this behavior is consistent with a gap energy near 568 cm^{-1}, i.e., 8.7 kT_c in $HgBa_2CuO_{4+\delta}$ and constitutes a first estimate of the superconducting gap in this material. The Raman tensor elements for the assigned A_{1g} and E_g modes are given in absolute units.

I. INTRODUCTION

The high superconducting transition temperatures recently observed[1–4] in the $HgBa_2Ca_{n-1}Cu_nO_{2+2n+\delta}$ series (denoted Hg-1201, Hg-1212, Hg-1223 in the following), especially under high pressure, have produced great interest in their structural and physical properties. The unit cells of the ideal defectless structures of these superconductors were found[5,6] to have tetragonal D_{4h} symmetry with space group $P4/mmm$ (D^1_{4h}). Phonons are important in this investigation in the following respects. Due to the observed electron-phonon interaction, the role of phonons, if any, in the superconducting mechanism needs to be clarified. The phonon self-energy effects in the superconducting state[7–12] in $YBa_2Cu_3O_7$ and $Bi_2Sr_2CaCu_2O_8$ (denoted Y-123 and Bi-2212) are well known. They reflect a redistribution of the density of electronic excitations with varying temperature and are usually, but not always, induced by the appearance of superconductivity. Furthermore, the phonons, specifically their Raman-active subset, have been used for distinguishing superconducting phases, defects, and impurity phases. Some of these phases or defects are not as easy to detect with common structural probes. As a consequence of the rather low purity of the polycrystalline samples available at this time, the phonons intrinsic to the superconducting phase need to be identified and distinguished from those of nonsuperconducting impurity phases. Within the superconducting phase, substitutional and interstitial defects have been identified by neutron scattering.[6] The defects of these phases, like in $YBa_2Cu_3O_{7-\delta}$, seem to be important for the Hg-based high-T_c superconductors since T_c varies significantly with oxygen occupancy in the HgO planes in Hg-1201. Within the series $n = 1$–3, T_c is greater compared to the homologous series $TlBa_2Ca_{n-1}Cu_nO_{2+2n+\delta}$.[13] In addition, defects and impurities may play an important role in other basic physical properties, such as the electronic Raman continuum common also to other high-T_c superconductors.[14]

We present a systematic Raman investigation and assignment of phonons intrinsic to the superconducting Hg-1201 phase which is consistent with the polarization selection rules and the well-known Raman properties of other cuprate superconductors. Absolute Raman cross sections and Raman tensor phase factors for these modes are determined. In addition, the Raman spectra of HgO and $HgCaO_2$ are shown. Furthermore, we report the observation of an anomalous phonon self-energy effect occurring around T_c in Hg-1201.

II. EXPERIMENTAL DETAILS

A number of samples were synthesized from the constituent metal oxides BaO_2 and CuO by producing a precursor of Ba_2CuO_3, which was then sealed with HgO in a quartz ampule surrounded by a steel container under O_2 and reacted at 400 °C (4 days) and 800 °C (12 h) yielding $HgBa_2CuO_{4+\delta}$. The samples were subsequently oxygenated at 300 °C (4 h).

X-ray data consistently showed the presence of the Hg-1201 phase while no impurity phases were detected. Field cooled and zero-field cooled susceptibility data yielded a sharp (ΔT = 2 K) superconducting transition at 95 K with Meissner fractions of ~30%. In addition, impurity phases were produced intentionally by reacting HgO + 2BaO and HgO + CaO + 2BaO, i.e., the starting stoichiometries used for the synthesis of Hg-1201 and Hg-1212 except for CuO with the otherwise same procedure as used to synthesize the superconductor. The Raman spectra were taken with 5145 Å excitation in a subtractive triple spectrograph with a Raman microscope (spot size ~1 μm) and at low temperature using standard focusing and collection optics (spot size ~30 μm).

III. RESULTS AND DISCUSSION

Figure 1(a) shows the Raman spectra of polycrystalline HgO [space group $Pnma$ (D_{2h}^{16})] with prominent peaks at 567 cm^{-1} and 332 cm^{-1}, and Fig. 1(c) that of $HgCaO_2$ (peaks at 670 cm^{-1} and 240 cm^{-1}) in parallel (vv) and crossed (hv) incident and scattered polarizations. The latter spectra ($HgCaO_2$) are identical with those obtained from the HgO + CaO + 2BaO starting stoichiometry (not shown) except for some admixture of HgO [Fig. 1(a)]. Figure 1(b) shows the spectra of the compound reacted with starting stoichiometry HgO + 2BaO. Due to their similarity to the $HgCaO_2$ spectra, and consistent with a low-frequency shift expected for heavier ions, $HgBaO_2$ (641 cm^{-1} and 196 cm^{-1}) with an admixture of HgO (332 cm^{-1}) is a possible candidate for these spectra. Since even trace amounts of impurities with large Raman cross sections can dominate the spectra obtained from x-ray clean superconducting phases, these investigations were performed to ensure proper assignments of the phonons intrinsic to the superconductor. The spectra of the superconducting material were found to be free of the known impurities Cu_2O, CuO, $BaCuO_2$, CaO, and $BaCO_3$.

Figure 2 shows the Raman spectra obtained from a rectangular crystallite (imbedded in the superconducting sample) of about 6×6 μm^2, with parallel edges and an optically clean specular surface. They are identical to the spectra obtained from multiple spots on the same and other Hg-1201 samples of high-phase purity and are thus

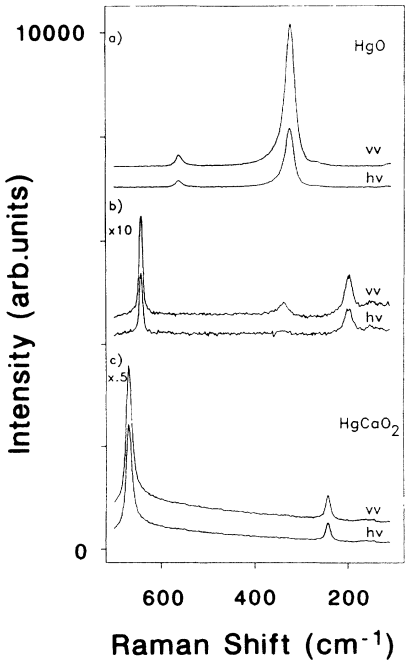

FIG. 1. Raman spectra of polycrystalline HgO (a), the compound (presumed $HgBaO_2$) resulting from reacting the starting stoichiometry HgO + 2BaO with the identical procedure as the superconductor (b), and polycrystalline $HgCaO_2$ (c) in parallel (vv) and crossed (hv) incident and scattered polarization.

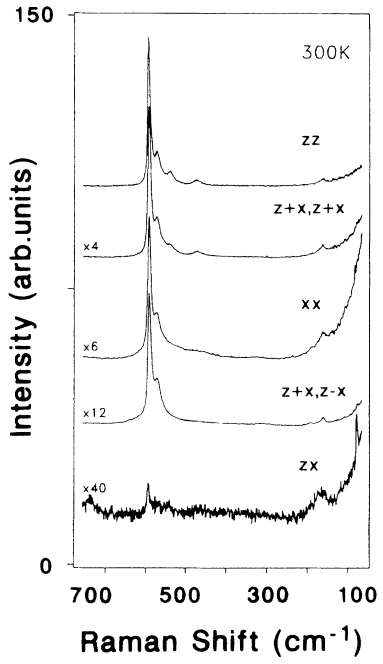

FIG. 2. Raman spectra taken on a rectangular $\sim 6 \times 6$ μm^2 single Hg-1201 crystallite with the microscope in parallel (zz; $z+x, z+x$, xx) and crossed polarizations (zx; $z+x, z-x$) for polarization vectors parallel (z, x) and at 45° ($z+x, z-x$) to the crystallite edges. The data are consistent with A_{1g} symmetry modes at 592 cm^{-1}, 568 cm^{-1}, and 161 cm^{-1} and E_g modes at 75 cm^{-1} and 168 cm^{-1} observed on a (010) [or (100)] surface. The intensities of the lower spectra have been enhanced by the indicated factors.

presumed to be intrinsic to the superconducting phase. The incident and scattered polarizations, denoted as z, x, $z+x$, and $z-x$, are taken to be parallel (z, x) and at 45° $(z+x, z-x)$ to the edges of the crystallite, with z, x presumed to correspond to two axes of the tetragonal structure for reasons supported by the selection rules discussed below. In what we label the zz polarization, prominent peaks at 592 cm^{-1} and 568 cm^{-1} and weak ones at 161 cm^{-1}, 530 cm^{-1}, and 470 cm^{-1} are observed. Except for the 530 cm^{-1} and the 470 cm^{-1} mode, which were not observed on all spots of the sample and presumably originate from defects, the same modes are present with lower intensity in xx polarization and are absent in the depolarized zx spectrum. In the $z+x, z+x$ and $z+x, z-x$ polarized and depolarized spectra, taken at 45° to the edges of the crystallite, the same modes are observed with similar relative intensities but larger depolarization ratios. The zx depolarized spectrum shows, in addition, a weak peak at 75 cm^{-1} (also present in $z+x, z+x$ polarization) and a broad one [full width at half maximum (FWHM) 22 cm^{-1}] at 168 cm^{-1} which cannot be assigned to polarization leakage from the 161 cm^{-1} mode (FWHM 10 cm^{-1}).

A factor group analysis of the ideal tetragonal $HgBa_2CuO_{4+\delta}$ structure yields four Raman-allowed modes, two of A_{1g} (z-direction displacement) and two of E_g (x-direction) symmetry involving vibrations of the apical O(2) oxygen and Ba ions as shown in Table I. The

TABLE I. Classification of the Raman-active modes in the ideal tetragonal $HgBa_2CuO_4$ structure with atomic sites specified in Wyckoff notation. The oxygen sites are labeled in c-axis direction starting from the CuO_2 plane. The dotted lines indicate Raman inactivity.

Site	Atom	$HgBa_2CuO_4$
$1a$	Cu	....
$2f$	O(1)	....
$2h$	Ba	$A_{1g}+E_g$
$2g$	O(2)	$A_{1g}+E_g$
$1b$	Hg	....

observed polarization behavior requires the assignment of A_{1g} symmetry to all modes with the exception of the zx-polarized modes, which have E_g symmetry.

In principle, a series of measurements for various incident and scattered polarizations allow the determination of the orientation of such a crystallite. Guided by the experience with other cuprate materials, we first considered the possibility of the platelets having an a-b surface, i.e., a (001) surface with a high-frequency mode involving the apical oxygen and a low-frequency one related to Ba vibrations. This assumption contradicts, however, the polarization behavior presented in Fig. 2, in particular the large Raman signal,[15] and hence Raman polarizability, obtained for the apical-oxygen vibration when excited parallel to one of the crystallite edges, but not the other (notice that their intensities differ by a factor of 6). On the other hand, if we assume the surface to be (010) [or (110)], the relative strengths can be understood rather well: They arise from a large zz polarizability of the apex oxygen, as is known from other superconductors.[15]

Group theory predicts the following relative strengths for the various phonon Raman tensors in D_{4h} symmetry (for (010) and [(110)] surfaces):

(1) parallel to one edge and $\hat{\mathbf{e}}_s \parallel \hat{\mathbf{e}}_i$ (A_{1g} modes),

$$I_1 = |c|^2, \qquad [|c|^2];$$

(2) parallel to the other edge and $\hat{\mathbf{e}}_s \parallel \hat{\mathbf{e}}_i$ (A_{1g} modes),

$$I_2 = |a|^2, \qquad [|a|^2];$$

(3) as (1) and (2) but $\hat{\mathbf{e}}_s \perp \hat{\mathbf{e}}_i$ (E_g modes),

$$I_3 = |e|^2, \qquad [|e|^2];$$

(4) parallel to a diagonal and $\hat{\mathbf{e}}_s \parallel \hat{\mathbf{e}}_i$ (A_{1g}, E_g),

$$I_4 = \frac{1}{4}|a+c|^2 + |e|^2, \qquad \left[\frac{1}{4}|a+c|^2 + |e|^2\right];$$

(5) as (4) but $\hat{\mathbf{e}}_s \perp \hat{\mathbf{e}}_i$ (A_{1g}),

$$I_5 = \frac{1}{4}|a-c|^2, \qquad \left[\frac{1}{4}|c|^2 + \frac{1}{2}|e|^2\right].$$

Here $\hat{\mathbf{e}}_s$ and $\hat{\mathbf{e}}_i$ denote the unit vectors of the incident and scattered polarization and a, c, e are the $R_{xx} = R_{yy}$, R_{zz}, and R_{xz} Raman tensor elements of A_{1g}, A_{1g}, E_g symmetry modes, respectively. Evaluating I_i from the areas under the experimental peaks, we find the experimental Raman tensors with complex elements for the modes of A_{1g} symmetry:

$$\overleftrightarrow{R}_{592} = \eta_1 \begin{pmatrix} 0.4\times e^{i} & & \\ & 0.4\times e^{i} & \\ & & 1 \end{pmatrix},$$

$$\overleftrightarrow{R}_{568} = \eta_2 \begin{pmatrix} 0.4\times e^{i} & & \\ & 0.4\times e^{i} & \\ & & 1 \end{pmatrix},$$

$$\overleftrightarrow{R}_{161} = \eta_3 \begin{pmatrix} 0.7\times e^{i0.8} & & \\ & 0.7\times e^{i0.8} & \\ & & 1 \end{pmatrix}.$$

Here we have normalized all tensor elements to the zz component of the respective mode. An estimate of the birefringence effects made using the optical constants for Y-123 suggests that the phases of the Raman tensor elements have an accurancy of only $\pm 30\%$. We have determined the absolute values for these tensor elements by comparing the Raman signal under identical conditions with Y-123, where absolute scattering strengths are known.[15] Using $S/(\hbar\omega)^4 = |\hat{\mathbf{e}}_s \cdot \overleftrightarrow{R} \cdot \hat{\mathbf{e}}_i|^2$ for the Raman efficiency at 514 nm in units of $(\mathrm{eV}^{-4}\,\mathrm{cm}^{-1}\,\mathrm{sr}^{-1})$ we find $\eta_1 = 0.005$, $\eta_2 = 0.0035$, $\eta_3 = 0.0012 \pm 30\%$ compared to $\eta = 0.0029$ for the apical-oxygen mode in Y-123. We have not corrected for a possible difference in the optical absorption depth or index of refraction of Y-123 and $HgBa_2CuO_{4+\delta}$ since the dielectric functions of the latter are not yet known. The relatively small value of the xx component for all $\overleftrightarrow{R}$ explains the results of Ren *et al.*[16] who did not observe a signal perpendicular to their supposed c axis. For $\hat{\mathbf{e}}_s \parallel \hat{\mathbf{e}}_i$ we calculate I_{xx}/I_{zz} to be 0.16, 0.16, and 0.5 for the 592 cm^{-1}, 568 cm^{-1}, and 161 cm^{-1} modes, respectively.

The assumption of a (010) surface, which produces good agreement between group theory and the observed A_{1g} mode intensities [as opposed to the assumption of a (110) surface], implies that the zx spectrum should only display modes of E_g symmetry. E_g modes are predicted with the same intensity in $x+z, x+z$ polarization and are Raman forbidden in the zz and xx spectra. The 75 cm^{-1} and 168 cm^{-1} (FWHM 22 cm^{-1}) modes in the zx spectrum are in good agreement with these selection rules while the observed 592 cm^{-1} zx mode is not. However, the strength of this mode can be used to set an upper limit of less than 1% to the polarization leakage from A_{1g} modes. Using Y-123 as a standard yields the following absolute Raman tensor elements for the 75 cm^{-1} and 168 cm^{-1} modes (no phase information can be obtained):

$$\overleftrightarrow{R}_{75} = 0.001 \begin{pmatrix} & 0.3 \\ 0.3 & \end{pmatrix},$$

$$\overleftrightarrow{R}_{168} = 0.001 \begin{pmatrix} & 0.5 \\ 0.5 & \end{pmatrix}.$$

The near coincidence of the A_{1g} mode at 161 cm^{-1} (FWHM 10 cm^{-1}) and the 168 cm^{-1} (FWHM 22 cm^{-1}) E_g mode was confirmed with a high signal-to-noise Raman spectrum on a different crystallite resolving a superposition of both peaks. This is consistent with a presumed [101] direction of $\hat{e}_s$ and $\hat{e}_i$, where modes of A_{1g} and E_g symmetry are Raman allowed simultaneously.

The only low-frequency mode of A_{1g} symmetry (161 cm^{-1}) can be clearly assigned to the Ba vibration. Its relatively high frequency, as compared to the $YBa_2Cu_3O_7$ (116 cm^{-1}) and most other cuprates, may result, in part, from the absence of coupling to neighboring Raman-allowed A_{1g} modes of higher frequency (such as the A_g Cu mode of Y-123) and of the close proximity of the two Ba atoms, separated by only a single CuO_2 plane.

From the two candidates an assignment of the remaining single A_{1g} mode predicted for the ideal defectless Hg-1201 structure is possible. The two strongest high-frequency modes of A_{1g} symmetry, observed at 592 cm^{-1} and 568 cm^{-1}, display a nearly constant integrated intensity ratio of $\sim$2, despite the large intensity variations measured in different polarizations. This rules out assigning either of them to motion of the O(4) and O(3) oxygen defects in the Hg plane, as their weak bonding in the c direction precludes high-frequency modes and ab-plane motion would produce varying intensity ratios to the apical oxygen c-axis mode. The presence of an oxygen defect in the Hg plane, however, breaks the symmetry of the CuO_2 plane, thereby permitting Raman activity of the Cu(1) ion and producing a frequency-shifted apical-oxygen mode. The other remaining candidate for the additional high-frequency mode involves the identified Cu-substitutional defect (on a Hg site).[6] The 1.97 Å O-Hg-O bond length in Hg-1201 is smaller than in HgO ($Pnma$) (2.05 Å), thus requiring a higher mode frequency than the one observed at 567 cm^{-1}. Conversely, the O-Cu-O dumbell sections of 1.92 Å bond length[17] in the linear chains in Y-124 produce a mode[18] at 600 cm^{-1}, thus requiring a lower mode frequency of the corresponding O-Cu_{defect}-O mode with presumed 1.97 Å bond length. As a result, an assignment of the 592 cm^{-1} and 568 cm^{-1} peaks to the apical-oxygen modes of the ideal Hg-1201 structure and of a Cu-substitutional defect on a Hg site, respectively, is consistent with these bond length considerations and also with the ionic radii ($Cu^{2+} \approx 0.56$ Å, $Hg^{2+} \approx 1.1$ Å).[19,20] Furthermore, the integrated Raman intensity is similar to the one of the corresponding 500 cm^{-1} apical-oxygen mode in Y-123 single crystals obtained in zz polarization under identical conditions. The high Raman intensity of the Cu_{defect} apical-oxygen mode resulting from only 10% of the Hg sites of the ideal structure may result from the well-known fact that the O^{--} Raman polarizability diverges with ionic volume[21] (a larger ionic volume is permitted by the smaller Cu ion). Similarly, in $Nd_{2-x}Ce_xCuO_4$ a strong high-frequency vibrational mode at 581 cm^{-1} is produced with small (x = 0.2) Ce concentrations.[22] Another possibility is a higher than 10% Cu $\leftrightarrow$ Hg substitution near the surface (laser penetration depth $\sim$700 Å in Y-123). An unambiguous distinction of the A_{1g}-like defect mode assignment is not possible based on the available data. The small linewidth of the 592 cm^{-1} apical-oxygen mode may result from the coincidence of its phonon decay channel with a minimum in the two-phonon density of states available for anharmonic decay. A minimum is more likely to occur in structures with fewer phonon branches.[23]

For E_g symmetry two sets of modes are predicted for the ideal structure, one involving Ba and the other the apical oxygens. The 75 cm^{-1} peak is in good agreement with the Ba E_g mode of Y-123 observed at $\sim$90 cm^{-1} and lattice dynamics calculations yielding $\sim$81 cm^{-1} for Tl-1122 and 72 cm^{-1} for Tl-1223.[24] The 168 cm^{-1} peak can be assigned to the remaining predicted E_g mode involving a-axis motion of the apical oxygens. In orthorhombic Y-123 the corresponding B_{2g} mode was observed[25] at 210 cm^{-1} and its frequency was found to decrease to 196 cm^{-1} in Nd-123 (Ref. 26) due to a larger ionic radius (i.e., 1.1 Å). In Hg-1201 the greater apical-oxygen bond length must lead to a further significant reduction of the frequency in agreement with the 168 cm^{-1} observation and also E_g-mode predictions from shell model calculations[27] of 197 cm^{-1} and 94 cm^{-1}.

The 568 cm^{-1} A_{1g}-like mode displays an anomalous behavior of its frequency and linewidth below T_c. Figure 3 shows the temperature dependence of the 592 cm^{-1} and

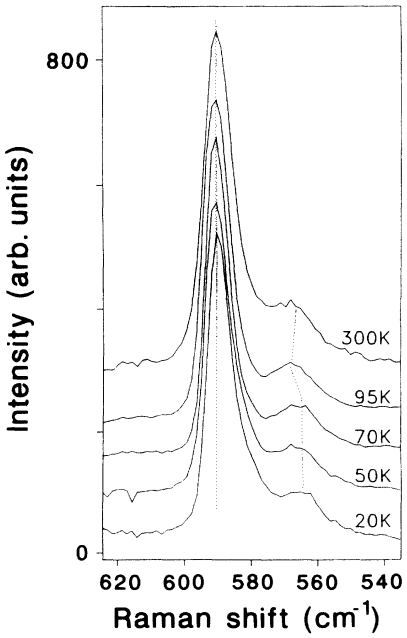

FIG. 3. Temperature dependence of the polarized Raman spectra of the 592 cm^{-1} and 568 cm^{-1} apical-oxygen modes of A_{1g} symmetry. The 568 cm^{-1} A_{1g}-like mode displays an abrupt $\sim$3 cm^{-1} mode softening below T_c while the 592 cm^{-1} mode behaves normally.

568 cm^{-1} apical-oxygen modes. Between 300 K and 95 K both modes (and the 161 cm^{-1} Ba A_{1g} mode) display the normal slight shift to higher frequencies and a linewidth narrowing. Below T_c, however, the 568 cm^{-1} mode displays an abrupt mode softening of ~3 cm^{-1} visible in the raw data (Fig. 3). At the same time the 592 cm^{-1} mode (and the 161 cm^{-1} Ba A_{1g} mode) remains effectively unchanged in frequency and linewidth. This anomalous phonon self-energy effect observed in the superconducting state is likely related to electron-phonon coupling, as no structural phase transition is known for Hg-1201 at low temperature[6] and anharmonic phonon-phonon coupling should be monotonic when crossing T_c. However a ferroelastic phase transition or Jahn-Teller distortion at or near T_c as a result of the small ionic radius of the Cu_{defect} ion cannot be ruled out. Detailed frequency and linewidth data for the 568 cm^{-1} mode softening were derived from least-square fits of Lorentzians to all low-temperature spectra and are shown in Fig. 4. The adjacent asymmetric 592 cm^{-1} modes were fitted with Fano line shapes or alternatively, with two Lorentzians (592 + 587 cm^{-1}), to allow for an interference with the electronic continuum or relaxation of the $q \approx 0$ selection rule due to reduced symmetry of the crystal, with the latter producing the best fits. Figure 4(a) displays the abrupt 2.5 cm^{-1} mode softening of the 568 cm^{-1} mode below T_c. The linewidth behavior in the superconducting state [Fig. 4(b)] is similarly anomalous. Below 100 K an abrupt broadening by ~3 cm^{-1} is observed followed by a narrowing of about 2 cm^{-1} between 70 K and 10 K. In this respect the phonon anomaly below T_c is similar to that observed for the Y-123 B_{1g}-like mode.[8]

Phonon anomalies related to electron-phonon coupling have been observed in many other cuprate superconductors. To date it is not clear if phonons play a special role in the superconducting mechanism, although the isotope effect strongly suggests it.[28] If the softening and broadening of Fig. 4 is used as a probe of the redistribution of the electronic states interacting with the phonons, detailed information on the electronic system can be extracted.[29] Specifically, if the temperature-dependent renormalization of the electronic continuum states, which presumably causes the phonon anomaly, is a result of the appearance of a superconducting gap, the softening of such a high-frequency phonon would require the gap to be near 570 cm^{-1}, i.e., about $8.7kT_c$. This would constitute the highest reported superconducting gap determined from phonon softening of Raman-active modes; such a softening has, however, been observed for the ir-active modes of Y-123 and Y-124 near that frequency.[11]

In summary, we have presented polarized Raman spectra of a single crystallite of $HgBa_2CuO_{4+\delta}$ and temperature-dependent spectra of polycrystalline samples. The results yield three modes obeying A_{1g} selection rules and two modes of E_g symmetry, which are assigned to the two predicted A_{1g} and E_g modes of the ideal structure, and one mode of A_{1g}-like symmetry associated with the Cu-Hg substitutional or oxygen defect in the Hg plane, respectively. In the superconducting state an anomalous abrupt mode softening and line broadening of the mode at 568 cm^{-1} are observed. This behavior is indicative of the electron-phonon interaction and if produced by the opening of a superconducting gap, requires its energy to be near $8.7kT_c$.

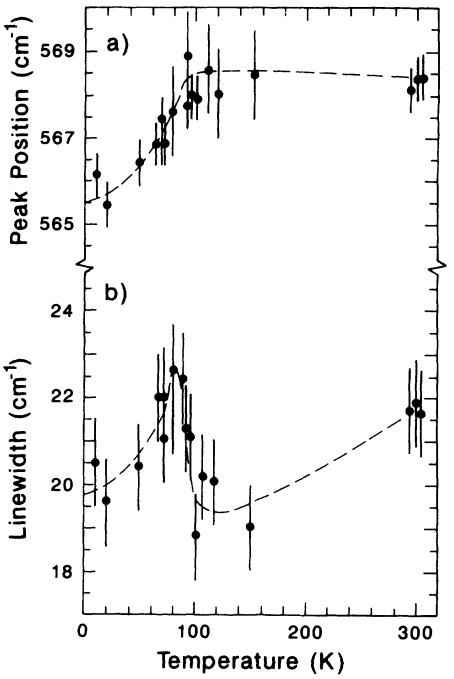

FIG. 4. Behavior of the frequency and linewidth (FWHM) of the 568 cm^{-1} mode in Hg-1201. Mode softening and broadening of about 3 cm^{-1} followed by subsequent narrowing of ~2 cm^{-1} is observed in the superconducting state.

ACKNOWLEDGMENTS

We are indebted to C. Hochrathner, H. Hirt, M. Siemers, and P. Wurster for expert technical help. We thank W. Reichardt for communicating to us the results of his calculation prior to publication. One of the authors (M.C.K.) would like to thank the Max-Planck-Institut für Festkörperforschung for financial support and its hospitality.

* Permanent address: IBM, San Jose, CA 95193.

[1] S.N. Putlin, E.V. Antipov, O. Chmaissem, and M. Marezio, Nature **362**, 226 (1993).

[2] E.V. Antipov, S.M. Loureiro, C. Chaillout, J.J. Capponi, P. Bordet, J.L. Tholence, S.N. Putlin, and M. Marezio, Physica C **215**, 1 (1993).

[3] A. Schilling, O. Jeandupeux, J.D. Guo, and H.R. Ott, Physica C **216**, 6 (1993).

[4] L. Gao, Z.J. Huang, R.L. Meng, J.G. Lin, F. Chen, L. Beauvais, Y.Y. Sun, Y.Y. Xue, and C.W. Chu, Physica C

213, 261 (1993).
[5] O. Chmaissem, Q. Huang, E.V. Antipov, S.N. Putlin, M. Marezio, S.M. Loureiro, J.J. Capponi, J.L. Tholence, and A. Sautoro, Physica C **217**, 265 (1993).
[6] J.L. Wagner, P.G. Radaelli, D.G. Hinks, J.D. Jorgensen, J.F. Mitchell, B. Dabrowski, G.S. Knapp, and M.A. Beno, Physica C **210**, 447 (1993).
[7] R.M. Macfarlane, H.J. Rosen, and H. Seki, Solid State Commun. **63**, 831 (1987).
[8] M. Krantz, H.J. Rosen, R.M. Macfarlane, and V.Y. Lee, Phys. Rev. B **38**, 4992 (1988).
[9] R.M. Macfarlane, M.C. Krantz, H.J. Rosen, and V.Y. Lee, Physica C **162-164**, 1091 (1989).
[10] B. Friedl, C. Thomsen, and M. Cardona, Phys. Rev. Lett. **65**, 915 (1990).
[11] A.V. Litvinchuk, C. Thomsen, and M. Cardona, in *Physical Properties of High-Temperature Superconductors IV*, edited by D.M. Ginsberg (World Scientific, Singapore, in press).
[12] D. Leach, C. Thomsen, M. Cardona, L. Mihaly, and C. Kenziora, Solid State Commun. **88**, 457 (1993).
[13] S.S.P. Parkin, V.Y. Lee, A.I. Nazzal, R. Savoy, T.C. Huang, G. Gorman, and R. Beyers, Phys. Rev. B **38**, 6531 (1988).
[14] D. Reznik, S.L. Cooper, M.V. Klein, W.C. Lee, D.M. Ginsberg, A.A. Maksimov, A.V. Puchkov, I.I. Tartakovshii, and S.-W. Cheong, Phys. Rev. B **48**, 7624 (1993).
[15] E.T. Heyen, S.N. Rashkeev, I.I. Mazin, O.K. Andersen, R. Liu, M. Cardona, and O. Jepsen, Phys. Rev. Lett. **65**, 3048 (1990).
[16] Y.T. Ren, H. Chang, Q. Xiong, Y.Q. Wang, Y.Y. Sun, R.L. Meng, Y.Y. Xue, and C.W. Chu, Physica C **217**, 273 (1993).
[17] P. Marsh, R.M. Flemming, M.L. Mandich, A.M. DeSantolo, J. Kwo, M. Hong, and L.J. Martinez-Miranda, Nature **334**, 141 (1988).
[18] M.C. Krantz, H.J. Rosen, J.Y.T. Wei, and D.E. Morris, Physica C **162-164**, 1089 (1989).
[19] A similar assigment for the 592 cm^{-1} but not the 568 cm^{-1} structure is suggested in Refs. 16 and 20 from unpolarized data.
[20] N.H. Hur, H.G. Lee, J.H. Park, H.S. Shin, and I.S. Yang, Physica C **218**, 365 (1993).
[21] J.R. Tessman, A.H. Kahn, and W. Shockley, Phys. Rev. B **92**, 890 (1953).
[22] E.T. Heyen, Ph.D. thesis, University of Stuttgart, 1991.
[23] This is consistent with preliminary Raman results on Hg-1223 where no narrow linewidth was observed for the apical oxygen mode.
[24] A.D. Kulkarni, F.W. de Wette, J. Prade, U. Schröder, and W. Kress, Phys. Rev. B **41**, 6409 (1990).
[25] K.F. McCarty, J.Z. Liu, R.N. Shelton, and H.B. Radousky, Phys. Rev. B **41**, 8792 (1990).
[26] B. Friedl, C. Thomsen, E. Schönherr, and M. Cardona, Solid State Commun. **76**, 1107 (1990).
[27] W. Reichardt (unpublished).
[28] J.P. Franck, J. Jung, M.A.K. Mohamed, S. Gygak, and G.I. Sproule, Phys. Rev. B **44**, 5318 (1991).
[29] R. Zeyher and G. Zwicknagl, Z. Phys. B **78**, 175 (1990).